

Article

# Mechanism for the Bio-Oxidation and Decomposition of Pentlandite: Implication for Nickel Bioleaching at Elevated pH

Jianzhi Sun <sup>1,2</sup> , Jiankang Wen <sup>1,2,\*</sup>, Biao Wu <sup>1,2</sup> and Bowei Chen <sup>2</sup>

<sup>1</sup> National Engineering Laboratory of Biohydrometallurgy, GRINM Resources and Environmental Technology Corporation Limited, Beijing 101407, China; beijing\_sunjianzhi@163.com (J.S.); angelwbiao@sina.com (B.W.)

<sup>2</sup> GRINM Group Corporation Limited, Beijing 100088, China; biohydrometallurgy@163.com

\* Correspondence: kang3412@126.com; Tel.: +86-010-60662781

Received: 28 February 2020; Accepted: 18 March 2020; Published: 23 March 2020



**Abstract:** This work investigated the effects of  $\text{Fe}^{3+}$ ,  $\text{H}^+$  and adsorbed leaching bacteria on the bioleaching of pentlandite. Collectively, an integrated model for the oxidation and decomposition of pentlandite was built to describe the behaviors of different components in a bioleaching system. Proton ions and ferric ions could promote the break and oxidation of Ni-S and Fe-S bonds. The iron-oxidizing microorganisms could regenerate ferric ions and maintain a high Eh value. The sulfur-oxidizing microorganisms showed significant importance in the oxidation of polysulfide and elemental sulfur. The atoms in pentlandite show different modification pathways during the bioleaching process: iron transformed through a  $(\text{Ni,Fe})_9\text{S}_8 \rightarrow \text{Fe}^{2+} \rightarrow \text{Fe}^{3+} \rightarrow \text{KFe}_3(\text{SO}_4)_2(\text{OH})_6$  pathway; nickel experienced a transformation of  $(\text{Ni,Fe})_9\text{S}_8 \rightarrow \text{NiS} \rightarrow \text{Ni}^{2+}$ ; sulfur modified through the pathway of  $\text{S}^{2-}/\text{S}_2^{2-} \rightarrow \text{S}_n^{2-} \rightarrow \text{S}^0 \rightarrow \text{SO}_3^{2-} \rightarrow \text{SO}_4^{2-}$ . During bioleaching, a sulfur-rich layer and jarosite layer formed on the mineral surface, and the rise of pH value accelerated the process. However, no evidence for the inhibition of the layers was shown in the bioleaching of pentlandite at pH 3.00. This study provides a novel method for the extraction of nickel from pentlandite by bioleaching at elevated pH values.

**Keywords:** pentlandite; bioleaching; bioleaching microorganisms; solution chemistry; surface modification; elevated pH

## 1. Introduction

As an indispensable raw metal material, nickel plays an important role in industry production. The industrial-scale application of nickel metal began over a hundred years ago, supporting the social development. Generally, economic nickel resource deposits are land-based, with about 40% in sulfide and 60% in laterite. Sulfide ore used to be the major resource for nickel, with a mature recovery technology of flotation, smelting, and electrowinning. However, with the over-consumption of high-grade sulfide ore and the decline in the discovery of new sulfide deposits, treatment for low-grade ore is of increasing interest.

Hydrometallurgy has been employed in the treatment of nickel laterite to avoid carbon emission and air pollution. Application of bio-hydrometallurgy has been extended to the extraction of nickel from sulfide ore. Several operational practices [1] of bio-heap leaching suggested that bio-hydrometallurgy could be a feasible technology for the recovery of nickel from low-grade sulfide ores. However, commercial applications are still facing technical challenges.

The biggest nickel bio-heap leaching plant was built at Talvivaara Sotakamo mine, and the project has been operating for nearly a decade. The ore only has commercial application value using bio-hydrometallurgy technology due to the low content of valuable metals. At the early stage of

heap leaching, extra acid consumption for pH maintenance is needed due to the rapid dissolution of pyrrhotite [2]. As the project continues, gradual bio-oxidation of sulfide minerals could lead to the accumulation of  $H^+$  [3]. Proton ions show remarkable influence on the leaching efficiency of both target metals and gangue minerals. Yet the mechanism for the influence of protons on the bioleaching of pentlandite remains unclear. Jinchuan Group Ltd. possesses the Jinchuan ore deposit which has about 400 Mt of low-grade nickel sulfide ore in Gansu province, China. Laboratory and pilot bioleaching tests were performed to solve the problem of lowering the grade [4,5]. Heap leaching suffered a high acid consumption of 710 kg/t (ore), which was caused by the presence of alkaline gangue minerals such as olivine, serpentine and chlorite. The dissolution of alkaline gangue minerals caused the accumulation of  $Mg^{2+}$  and  $Fe^{3+}$  in the leachate, challenging the leachate treatment system. Basically, the two examples above suggest that bio-hydrometallurgy is an economically feasible technology for low-grade nickel sulfide ore, but the promotion of bio-hydrometallurgy in nickel sulfide ore still faces challenges caused by the dissolution of gangue minerals.

As the most common nickel bearing sulfide mineral, pentlandite is the major target mineral in a nickel bio-heap leaching process. Therefore, the majority of publications about nickel bioleaching have been focusing on the bioleaching of pentlandite. Pentlandite is an acid-soluble mineral, and  $H^+$  ion show significant effects on the decomposition of the mineral structure. However, the release of metal ions from mineral particles leaves a metal-deficient (sulfur-rich) surface layer, which may inhibit the further dissolution of metal ions. Previous work has suggested that the addition of  $Cl^-$  could allow the formation of a more porous surface product and enlarge the recovery efficiency of nickel (Lu et al. [6]). However, a temperature of 85 °C and an oxygen pressure of 1 atm is necessary.  $Fe_2(SO_4)_3$  or  $FeCl_3$  was widely used as an efficient oxidant in the chemical leaching system [7,8]. Research [8] has shown that  $Fe^{3+}$  could only promote the release of  $Ni^{2+}$  during the early stage of chemical leaching. No obvious effect of ferric ions on the recovery efficiency was shown after 10 h of operation. Another defect of  $Fe^{3+}$  leaching is that excessive  $Fe^{3+}$  may result in a thicker jarosite layer on the mineral surface, which may be detrimental for mass transfer [9]. For low-grade ores, the chemical agitation leaching process has poor economic efficiency. Yet during a bioleaching process, the leaching bacteria could reduce the usage of  $Fe^{3+}$  [10] by regenerating  $Fe^{3+}$  via oxidizing  $Fe^{2+}$  released from pentlandite or produced in the reaction between  $Fe^{3+}$  and sulfide [11]. Meanwhile, the direct oxidation of leaching bacteria on sulfide was also noted [12].

Several studies have been focused on the effects of  $H^+$ ,  $Fe^{3+}$ , temperature and leaching bacteria on the bioleaching process [13,14]. The results implied that  $H^+$  and  $Fe^{3+}$  are of great benefit for the bio-oxidation and decomposition of sulfide minerals. However, low pH value and high concentration of  $Fe^{3+}$  could inhibit the growth of leaching bacteria. High temperature could promote the oxidation of the sulfur-rich layer, but it may be a risk to most leaching bacteria. High temperature will also accelerate the formation and precipitation of jarosite and cause the reduction of available  $Fe^{3+}$ . It is also noteworthy that  $Fe^{3+}$  precipitates completely at pH values above 3.0, generating  $H^+$ . Interactions between the above factors complicates the pentlandite bioleaching system. Hence, an intensive study about the bio-oxidation and decomposition of pentlandite during bioleaching is imperative.

This paper investigated the efforts of major components ( $Fe^{3+}$ ,  $H^+$ , leaching bacteria) on the oxidation and decomposition of pentlandite. Multiple technologies (ICP-OES, XRD, XPS and high-throughput sequencing) were used to reveal the mechanism for the oxidation and decomposition of pentlandite during bioleaching. As magnesium dissolution could be inhibited by raising the pH value of the leaching solution, it is of significant value to explore the possibility of extracting nickel from pentlandite at elevated pH values. Our work focuses on the bioleaching behaviors of pentlandite with both normal and elevated pH values, providing theoretical foundations for the application of bio-hydrometallurgy in the treatment of high-magnesium nickel sulfide ore.

## 2. Materials and Methods

### 2.1. Mineral and Bacteria

The original pentlandite used in this study was collected from Jinchuan Group Ltd. Other minerals were removed through flotation and magnetic separation. The samples were confirmed to exhibit high purity with only minor impurities through chemical and X-ray diffraction analysis. ICP studies indicated pentlandite contains 27.43% of Ni, 35.13% of Fe, 30.79% of S, 0.82% of Cu, 1.40% of Mg, 0.45% of Co and 0.91% of Si. The reagents were removed, and the purified pentlandite samples were dried and ground to fine powder guaranteeing that the particle size was less than 0.074 mm in size.

The mixed strain of bacteria applied in this study was obtained from National Engineering Laboratory of Biohydrometallurgy in Beijing, China. The strain mainly contained *Acidithiobacillus ferrooxidans* (70.65%), *Ferrimicrobium acidiphilum* (24.56%) and *Leptospirillum ferrooxidans* (4.13%). *Acidithiobacillus thiooxidans* was not detected due to the absence of sulfur-containing nutrients. The leaching bacteria was cultured in a 9K medium, which contained 3 g  $(\text{NH}_4)_2\text{SO}_4$ ,  $\text{K}_2\text{HPO}_4$  0.50 g, KCl 0.10 g,  $\text{Ca}(\text{NO}_3)_2$  0.01 g, and 44.22 g  $\text{FeSO}_4 \cdot 7\text{H}_2\text{O}$  per liter. The pH value was adjusted to 1.80 with 0.1M  $\text{H}_2\text{SO}_4$ .

### 2.2. Leaching Experiments

The chemical leaching of pentlandite was carried out in a 250 mL Erlenmeyer flask containing 100 mL sterilized water and 3 g of pentlandite. Before experiments, the pentlandite samples were sprayed with 95% ethanol and exposed to ultraviolet light. The pH value of the culture medium was initially adjusted to 1.0. The flask was placed in an orbital shaker incubator maintained at 150 rpm and 33 °C. The initial concentration of  $\text{Fe}^{3+}$  was 0, 1, 3, 5, 7 and 9 g/L separately. During the experiments, the evaporated water was compensated with sterilized ultra-pure water based on weight loss at one-day intervals. Samples of 2 mL were taken at two-day intervals for chemical analysis. During the chemical leaching experiments, 0.5% kanamycin was added to inhibit the growth of microorganisms.

The hydrogen/bioleaching tests of pentlandite were carried out using pH-stat batch stirred tank reacting system [15] (Figure 1). Eight grams of pentlandite was put into a 500 mL boiling flask containing 400 mL sterilized water. The pH of the solution in the tank was monitored by a computer connecting to a pH meter. The computer controlled two peristaltic pumps. The pH of the leaching system was maintained at a set point (2.00 or 3.00) with a fluctuation of  $\pm 0.05$  by adding 5% (vol/vol)  $\text{H}_2\text{SO}_4$  and/or 0.5 M  $\text{KHCO}_3$ . The stirring speed was set at 250 rpm, and the temperature was maintained at 33 °C by an Electro-Thermostatic Water Bath. The leaching bacteria were centrifuged at the logarithmic growth stage to avoid the interference of introducing ions. The initial bacteria density was  $1.5 \times 10^6$  cells/mL. During the experiments, the evaporated water was compensated with sterilized ultra-pure water based on weight loss at one-day intervals. Samples of 2 mL were taken at two-day intervals for chemical analysis. The bioleaching tests were carried out in duplicate, one of which was conducted for 8 days and the other for 16 days. At the end of each test, 2 g of the moist leached samples were collected and used for the DNA detection.

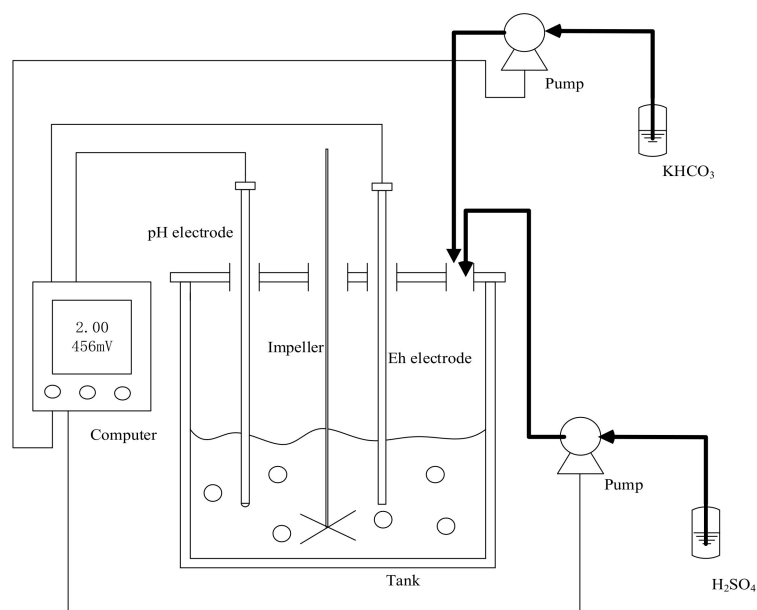


**Figure 1.** pH-stat batch stirred tank reacting system.

### 2.3. Analysis Methods

All solution samples were filtered by a cellulose acetate membrane (0.22  $\mu\text{m}$ ). The concentration of  $\text{Fe}^{2+}$  was titrated by potassium dichromate solution. The concentration of  $\text{Ni}^{2+}$  and total Fe (TFe) in solution was detected by ICP-OES (725-Agilent Technologies, Santa Clara, CA, USA). The Eh values in the slurries were measured using a Pt electrode with an Ag/AgCl reference electrode. Leached samples were characterized by X-ray diffraction (XRD). A scanning electron microscope (SEM; JSM-6510) was used to observe leached samples. X-ray photoelectron spectroscopy (XPS) tests were carried out with the model ESCALAB 250Xi (ThermoFisher Scientific, Waltham, MA, USA). Spectra were recorded at the constant pass energy of 20 eV and 0.1 eV/step using Al Ka X-ray source. Binding energies were referred to the C 1s level at 284.8 eV. XPS was used to delineate the evolution of Ni, Fe and S. The community DNA of adsorbed bacteria on the leached samples (250 mg) was extracted using E.Z.N.ATM Mag-Bind Soil DNA Kit (OMEGA, Norcross, GA, USA) according to the manufacture's protocol. The microbial communities of the leaching bacteria adsorbed on the leached samples were profiled using Illumina Miseq high-throughput platform [16].

## 3. Results

### 3.1. The Effect of Ferric Ions

#### 3.1.1. Solution Chemistry

The pH value in all tests reduced sharply from 1.00 to a range between 0.44 and 0.49, which was caused by the oxidation of sulfur species and the production of sulfuric acid (Figure 2). The leaching system with no initial adding of  $\text{Fe}^{3+}$  had the highest final pH value. The results showed that the decomposition of pentlandite was an acid-producing process. Overall, the Eh values in all solutions showed a downward trend at the early stage, followed by a relatively constant stage with an Eh value between 400 and 450 mV. Then, the Eh values increased constantly. At the final stage, the Eh value was maintained at a high level of around 550–600 mV.

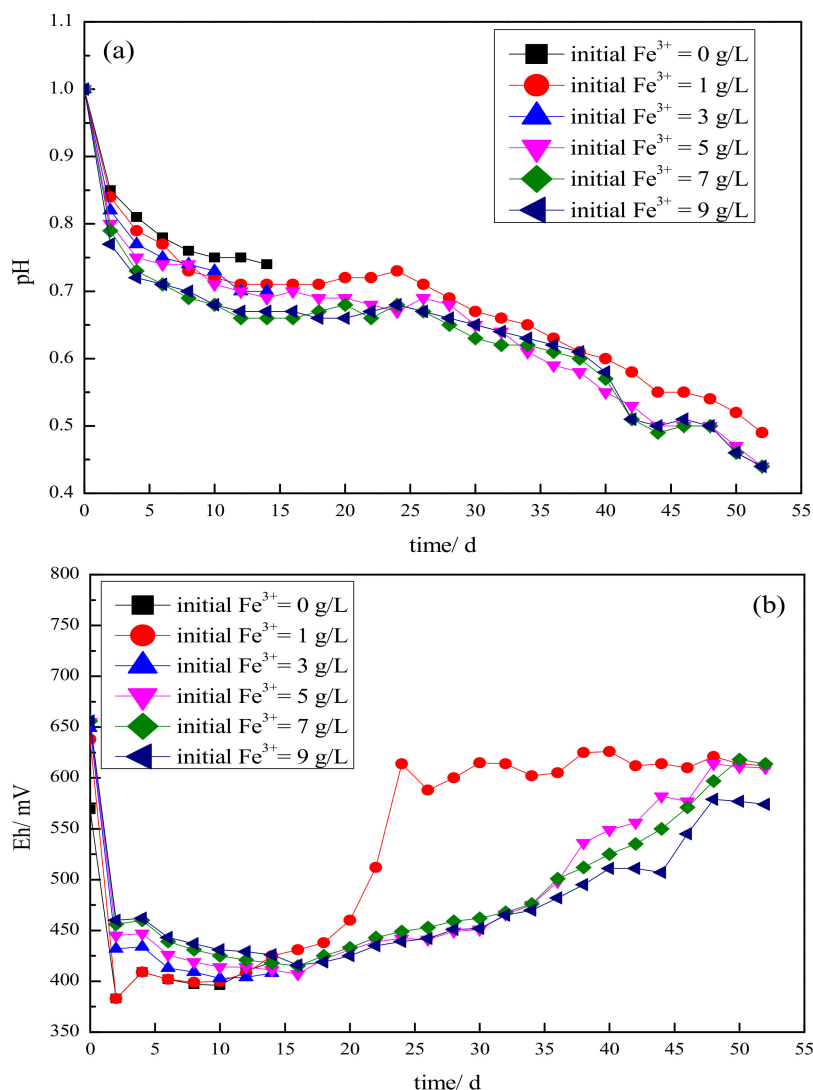


Figure 2. Changes in pH (a) and Eh (b) in solutions with time.

The Eh value in a leaching system with  $\text{Fe}^{3+}$  and  $\text{Fe}^{2+}$  as the dominant oxidation–reduction couples was highly correlated with the ratio of  $\text{Fe}^{3+}/\text{Fe}^{2+}$  [17]. The decrease of Eh values was caused by the decrease of  $\text{Fe}^{3+}$  and also the increase of  $\text{Fe}^{2+}$ . The changes in the concentrations of  $\text{Fe}^{2+}$  and  $\text{Fe}^{3+}$  could be divided into four stages throughout the leaching period (Figure 3). At the early stage (day 0–4), the concentration of  $\text{Fe}^{3+}$  showed a sharp decrease. In the meantime, the ferrous ions were released from the mineral rapidly. During the second stage (day 4–14), the concentrations of  $\text{Fe}^{3+}$  and  $\text{Fe}^{2+}$  were maintained at a stable range. At the third stage (day 14–38), the concentration of  $\text{Fe}^{2+}$  decreased gradually, indicating a reduction of the release of  $\text{Fe}^{2+}$  from pentlandite and consumption of  $\text{Fe}^{2+}$  during the oxidation reaction with oxygen. With the oxidation of  $\text{Fe}^{2+}$ , the concentration of  $\text{Fe}^{3+}$  went up gradually. At the final stage (day 38–52), the concentration of  $\text{Fe}^{3+}$  remained unchanged or increased slightly. The amount of  $\text{Fe}^{2+}$  was almost equal to zero, indicating the depletion of the  $\text{Fe}^{2+}$  released by pentlandite. Therefore, the Eh value increased sharply.

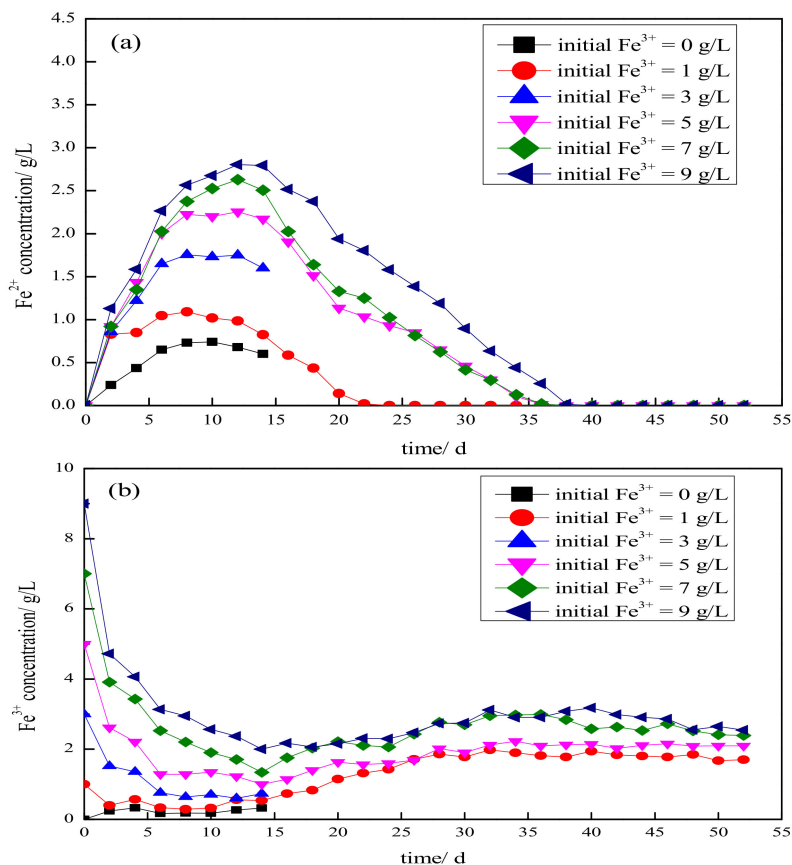


Figure 3. Changes in Fe<sup>2+</sup> (a) and Fe<sup>3+</sup> (b) in solutions with time.

The gradual increase of nickel leaching efficiency in all experimental tests confirmed an unhindered dissolution of Ni<sup>2+</sup> from pentlandite over time (Figure 4). Obviously, Fe<sup>3+</sup> accelerated the dissolution of Ni<sup>2+</sup> at the earlier stage (day 0–20). During the earlier stage, the highest nickel leaching efficiency was achieved with an initial Fe<sup>3+</sup> concentration of 5 g/L. However, as the leaching process went on, the promotion of Fe<sup>3+</sup> on the decomposition of pentlandite could be negligible, and some drawback was shown with an initial Fe<sup>3+</sup> concentration higher than 1 g/L. It is suggested that the addition of Fe<sup>3+</sup> might have some negative effect on the dissolution of Ni<sup>2+</sup> at the end of the leaching stage.

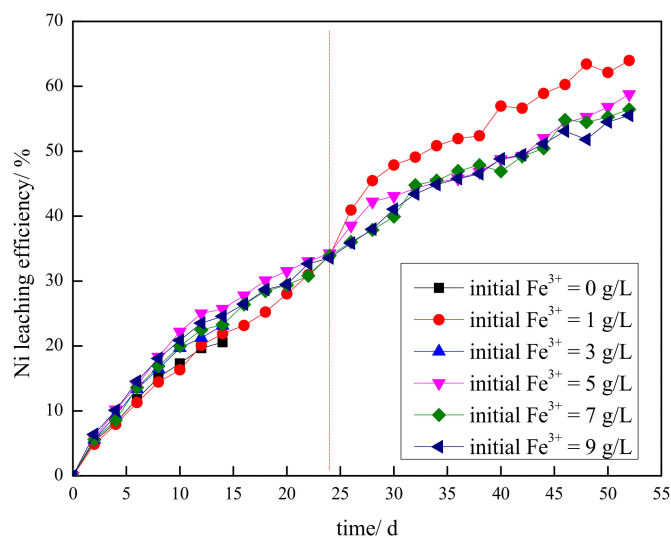
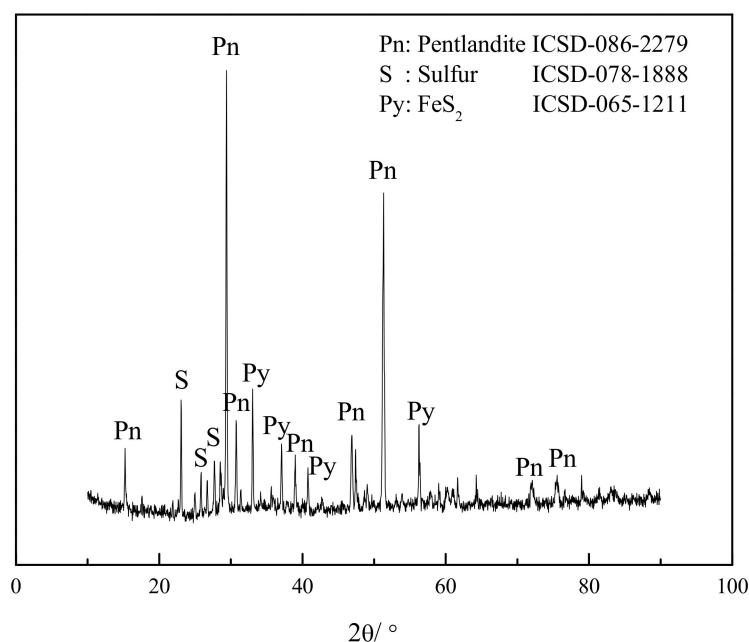


Figure 4. Changes in the Ni leaching efficiency with time.

### 3.1.2. Mineral Surface Modification

The formation of sulfur recorded the chemical oxidizing processes under the influence of ferric ions. Pyrite ( $\text{FeS}_2$ ) was identified as the intermediate mineral phase (Figure 5). Some other intermediate phases may not have been detected due to the limitation of X-ray diffraction technology.



**Figure 5.** XRD pattern of leached sample (leached for 52 days with an initial  $\text{Fe}^{3+}$  concentration of 7 g/L).

The sulfur species in the surface layer of leached samples comprises  $\text{S}^{2-}$ ,  $\text{S}_2^{2-}$ ,  $\text{S}_n^{2-}$ ,  $\text{S}^0$  and  $\text{SO}_4^{2-}$  (Table 1). After 14 days of leaching, the addition of  $\text{Fe}^{3+}$  had little effect on the composition of sulfur species on the mineral surface (Figure 6a,b) due to the low level of Eh value. However, as the reaction went on, the  $\text{S}_2^{2-}$  content changed from over a half to 38.72%, and  $\text{S}_n^{2-}$  changed from less than 20% to 31.31%. Besides,  $\text{SO}_4^{2-}$  was shown on the surface of the leached sample. The Fe 2p peaks of leached samples at 706.5–707.5 eV were assigned as  $(\text{Ni},\text{Fe})_9\text{S}_8$  or  $\text{FeS}_2$  (Figure 7). No peaks of Fe(III)-O were shown throughout the leaching process. The Ni 2p peaks of leached samples at 852.6 and 853.5 eV were assigned as  $(\text{Ni},\text{Fe})_9\text{S}_8$  and Ni-S respectively (Figure 8).

**Table 1.** Binding energy and full width at half maxima of sulfur specie in XPS profiles.

Analyzed Samples	$\text{S}^{2-}$		$\text{S}_2^{2-}$		$\text{S}_n^{2-}$		$\text{S}^0$		$\text{SO}_4^{2-}$	
	B.E.	FWHM	B.E.	FWHM	B.E.	FWHM	B.E.	FWHM	B.E.	FWHM
a	161.5	1.1	162.7	1.2	163.6	1.2	164.6	1.4	-	-
b	161.5	1.1	162.7	1.3	163.8	1.4	164.2	1.4	-	-
c	161.3	1.0	162.5	1.3	163.6	1.1	164.3	1.4	168.5	1.2

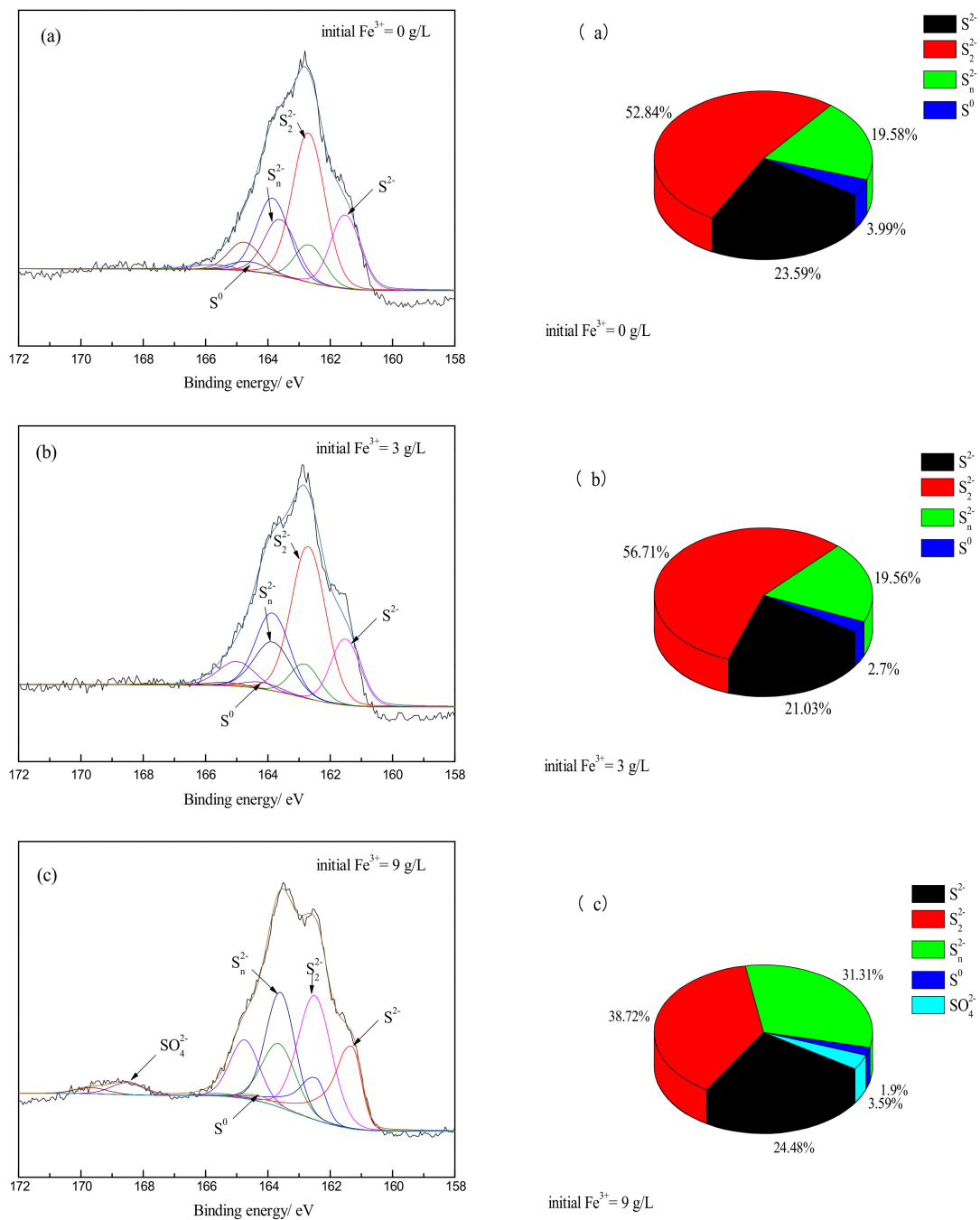


**Figure 6.** S 2p XPS spectra of leached samples with different conditions: (a) initial Fe<sup>3+</sup> = 0 g/L, leached for 14 days; (b) initial Fe<sup>3+</sup> = 3 g/L, leached for 14 days; (c) initial Fe<sup>3+</sup> = 9 g/L, leached for 52 days.

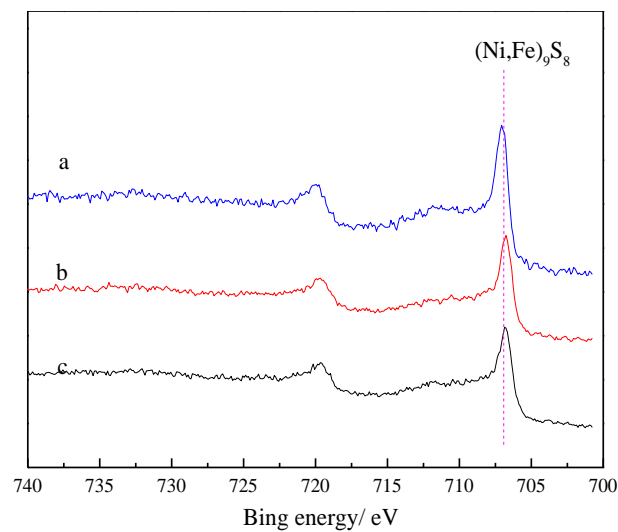


**Figure 7.** Fe 2p XPS spectra of leached samples with different conditions: (a) initial  $\text{Fe}^{3+} = 0$  g/L, leached for 14 days; (b) initial  $\text{Fe}^{3+} = 3$  g/L, leached for 14 days; (c) initial  $\text{Fe}^{3+} = 9$  g/L, leached for 52 days.

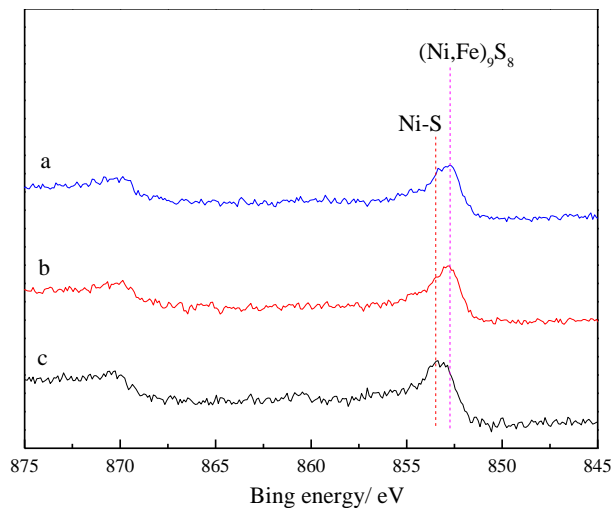


**Figure 8.** Ni 2p XPS spectra of leached pentlandite with different conditions: (a) initial  $\text{Fe}^{3+} = 0$  g/L, leached for 14 days; (b) initial  $\text{Fe}^{3+} = 3$  g/L, leached for 14 days; (c) initial  $\text{Fe}^{3+} = 9$  g/L, leached for 52 days.

### 3.2. The Effect of pH Value

#### 3.2.1. Solution Chemistry

It is indicated that the decrease of pH value is of benefit for the dissolution of  $\text{Fe}^{2+}$  and  $\text{Ni}^{2+}$  (Figure 9). The results suggested that hydrogen ions could provide a certain boost to the Eh value of the solution. It also promotes the dissolution of  $\text{Ni}^{2+}$  and  $\text{Fe}^{2+}$ . Due to the precipitation of  $\text{Fe}^{3+}$ , some drawback of  $\text{Fe}^{2+}$  leaching efficiency was shown during the later stage of leaching when hydrogen ions were scarce.

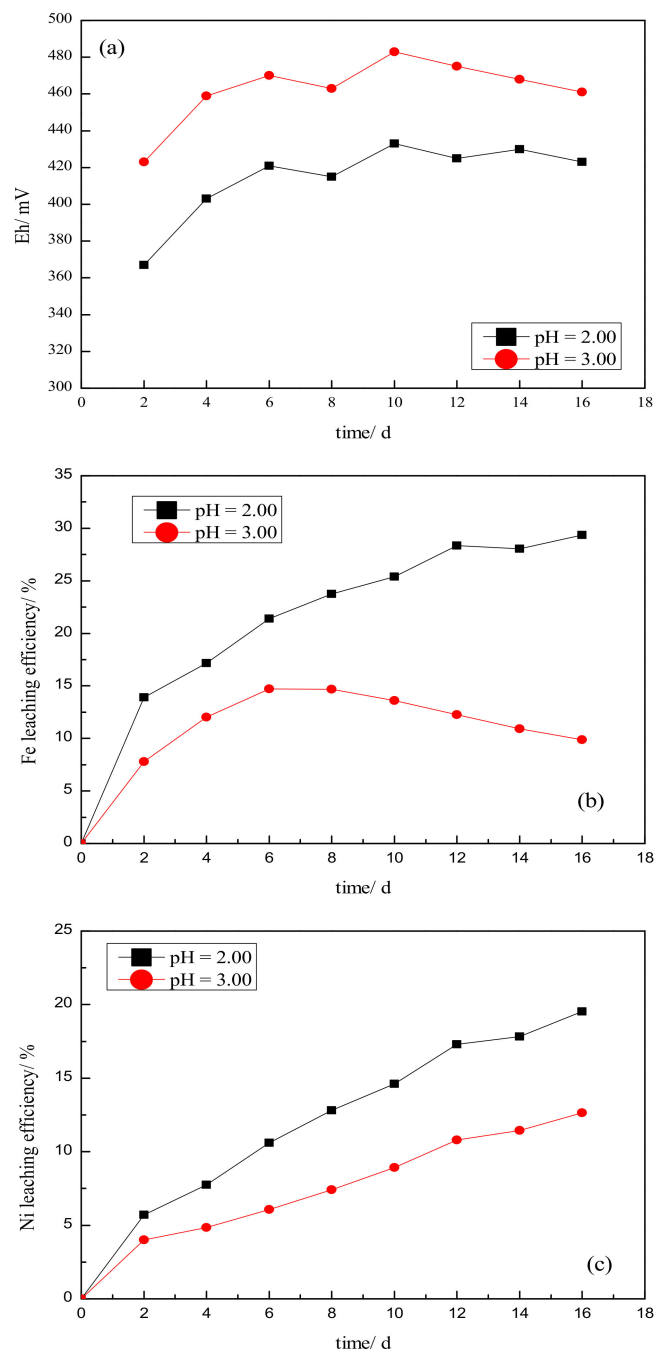


**Figure 9.** Changes in Eh (a), iron leaching efficiency (b) and nickel leaching efficiency (c) in solutions over time.

### 3.2.2. Mineral Surface Modification

A major difference of the sulfur species in the surface layer of leached samples was shown (Figure 10 and Table 2). The content of  $\text{SO}_4^{2-}$  increased nearly six-fold when the pH value increased from 2.00 to 3.00. Also, a significant increase of Fe(III)-O was detected (Figure 11).

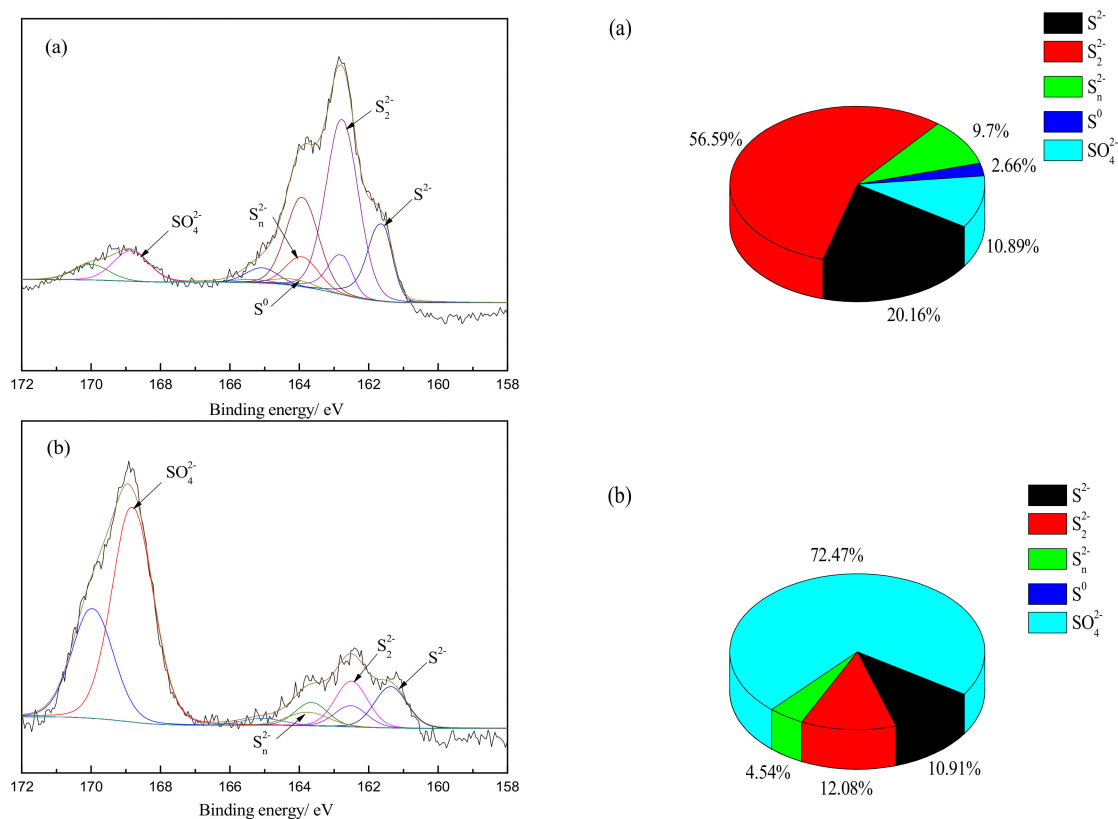


**Figure 10.** S 2p XPS spectra of leached pentlandite with different conditions: (a) pH = 2.00, leached for 16 days; (b) pH = 3.00, leached for 16 days.

**Table 2.** Binding energy and full width at half maxima of sulfur specie in XPS profiles.

Analyzed Samples	S <sup>2-</sup>		S <sub>2</sub> <sup>2-</sup>		S <sub>n</sub> <sup>2-</sup>		S <sup>0</sup>		SO <sub>4</sub> <sup>2-</sup>	
	B.E.	FWHM	B.E.	FWHM	B.E.	FWHM	B.E.	FWHM	B.E.	FWHM
a	161.6	1.1	162.8	1.1	163.9	1.2	164.2	1.4	168.8	1.2
b	161.4	1.1	162.5	1.1	163.8	1.4	164.2	1.5	168.8	1.4

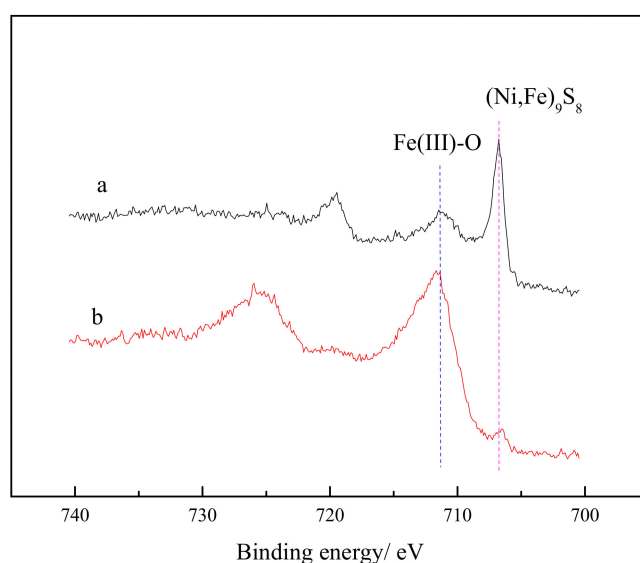


**Figure 11.** Fe 2p XPS spectra of leached pentlandite with different conditions: (a) pH = 2.00, leached for 16 days; (b) pH = 3.00, leached for 16 days.

### 3.3. The Effect of Leaching Bacteria

#### 3.3.1. Solution Chemistry

The bioleaching experiment of pentlandite was carried out with different constant pH values (Figure 12). During the experiment, a lower Eh value was shown with an elevated pH value. It stood to reason that the iron leaching efficiency was extremely low, as the oxidized  $\text{Fe}^{3+}$  precipitated under elevated pH values. It is worth noting that the nickel leaching efficiency was almost unaffected despite the low concentrations of  $\text{H}^+$  and  $\text{Fe}^{3+}$ .

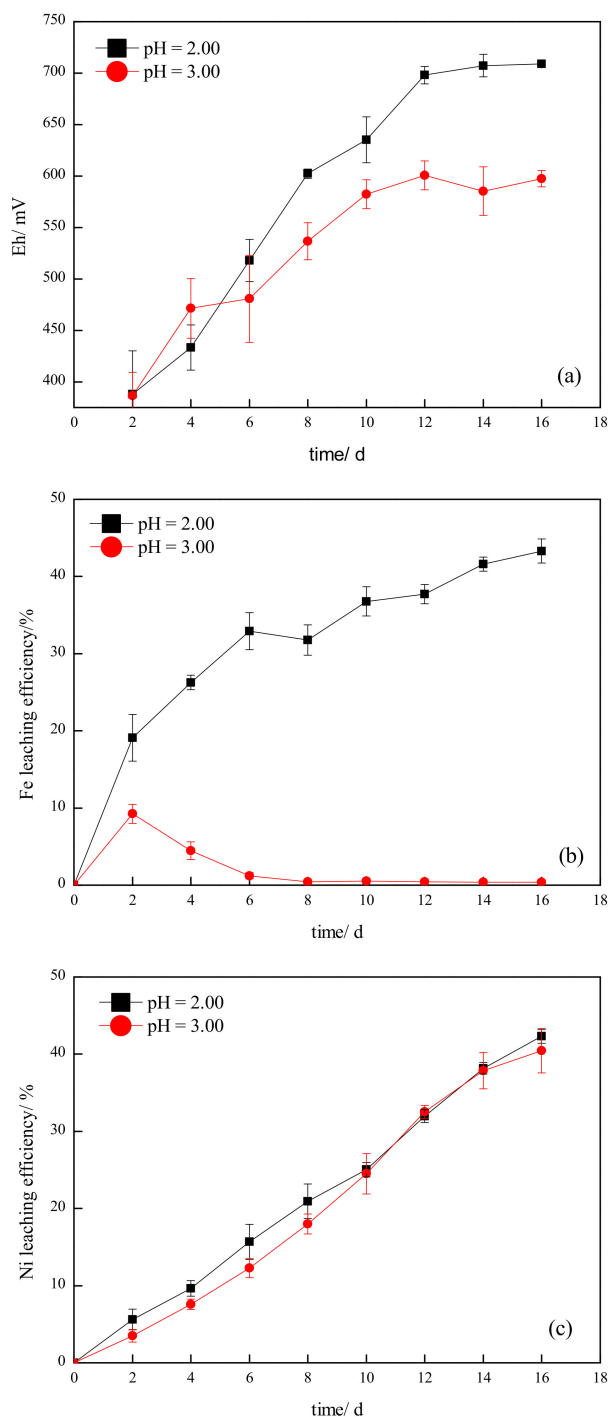


**Figure 12.** Changes in Eh (a), iron leaching efficiency (b) and nickel leaching efficiency (c) in solutions with time.

### 3.3.2. Mineral Surface Modification

According to the X-ray diffraction results in Figure 13, more elemental sulfur appeared in the later stage at pH 3.00 (Table 3). The micrographs of leached samples at different pH values are shown in Figure 14. At normal pH value (pH = 2.00), traces of corrosion were shown on the mineral surface. With the reaction going on, the mineral surface was covered with a loose produce layer. At elevated pH values (pH = 3.00), the generation rate of product layer was faster and it was denser. More  $\text{SO}_4^{2-}$  was shown on the surface of pentlandite particles at both pH values (Figures 15 and 16), different from the abiotic leaching process. It is clear that the increase of pH value accelerated the process. The results confirm the coverage by jarosite.

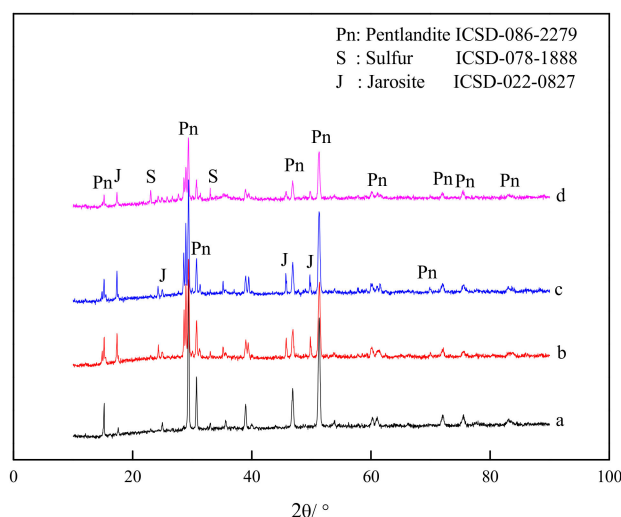


**Figure 13.** XRD pattern of filtered samples (a) pH = 2.00, leached for 8 days; (b) pH = 2.00, leached for 16 days; (c) pH = 3.00, leached for 8 days; (d) pH = 3.00, leached for 16 days.

**Table 3.** Binding energy and full width at half maxima of sulfur specie in XPS profiles.

Analyzed Samples	$\text{S}^{2-}$		$\text{S}_2^{2-}$		$\text{S}_n^{2-}$		$\text{S}^0$		$\text{SO}_4^{2-}$	
	B.E.	FWHM	B.E.	FWHM	B.E.	FWHM	B.E.	FWHM	B.E.	FWHM
a	161.5	1.1	162.6	1.26	163.6	1.4	164.6	1.6	168.6	1.5
b	161.5	1.1	162.9	1.3	163.6	1.4	164.4	1.5	168.7	1.3
c	161.4	1.1	162.5	1.1	163.6	1.4	164.6	1.6	168.9	1.3
d	161.4	1.1	162.6	1.3	163.6	1.4	164.5	1.6	168.8	1.3

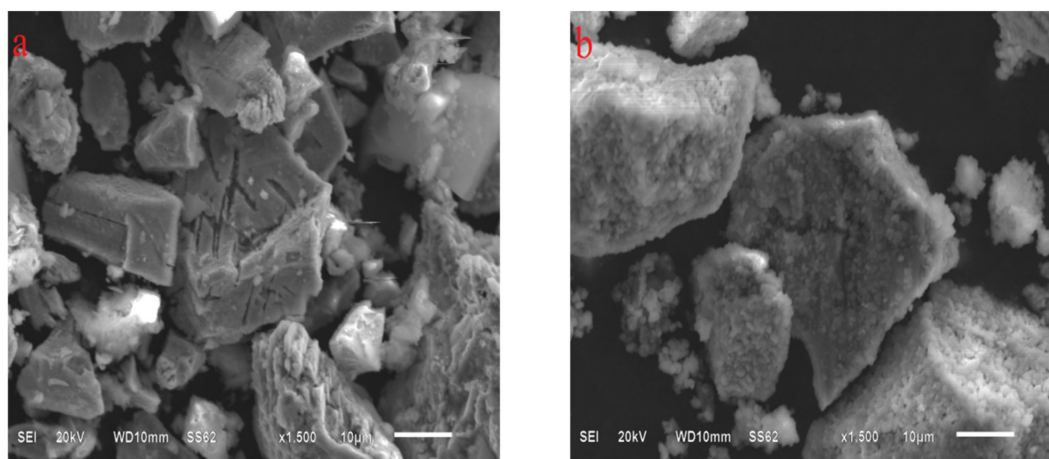


**Figure 14.** Cont.

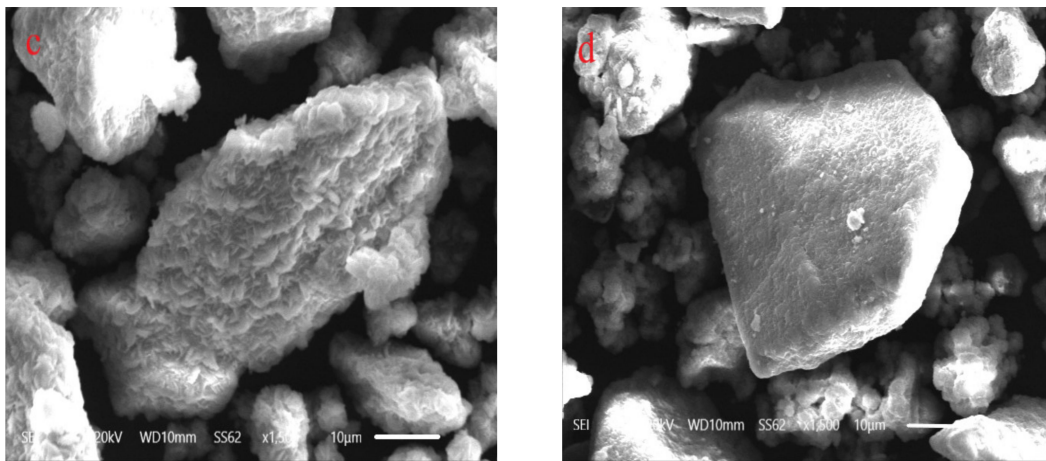


**Figure 14.** SEM micrographs of filtered samples: (a) pH = 2.00, leached for 8 days; (b) pH = 2.00, leached for 16 days; (c) pH = 3.00, leached for 8 days; (d) pH = 3.00, leached for 16 days.

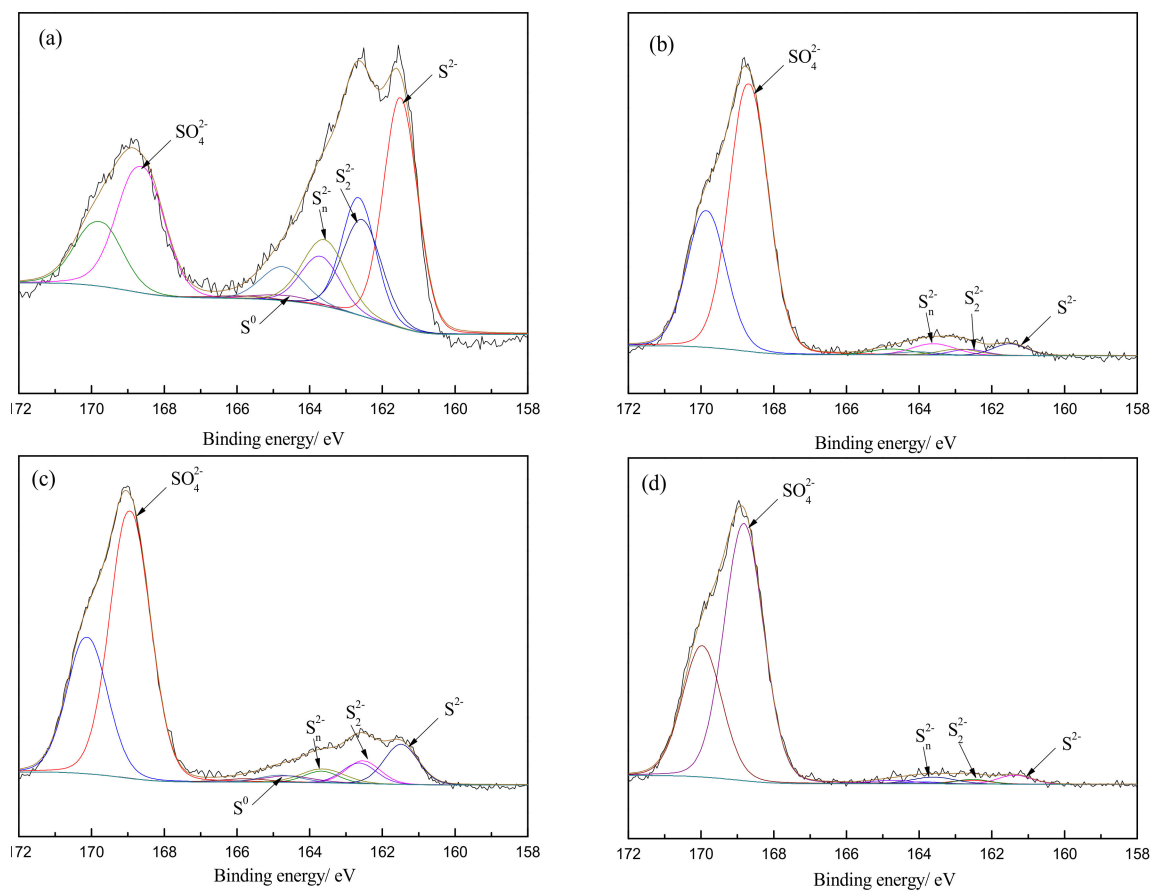


**Figure 15.** S 2p XPS spectra of leached pentlandite with different conditions: (a) pH = 2.00, leached for 8 days; (b) pH = 2.00, leached for 16 days; (c) pH = 3.00, leached for 8 days; (d) pH = 3.00, leached for 16 days).

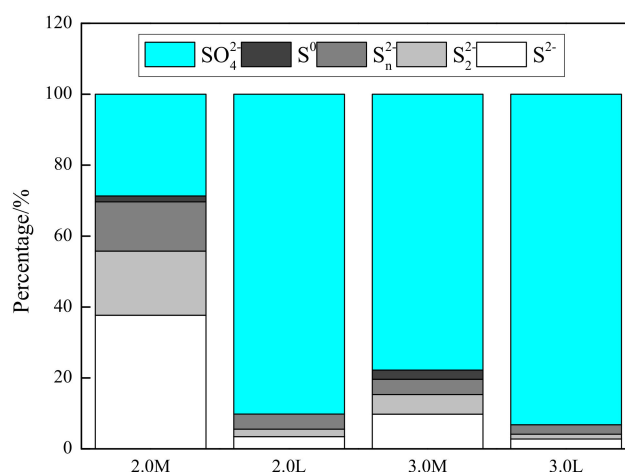


**Figure 16.** Contents of different sulfur species in the sulfur layer of pentlandite (2.0 M: pH = 2.00, leached for 8 days; 2.0 L: pH = 2.00, leached for 16 days; 3.0 M: pH = 3.00, leached for 8 days; 3.0 L: pH = 3.00, leached for 16 days).

### 3.3.3. Mineral Surface Microbial Community

The content of *Acidithiobacillus ferrooxidans* decreased from 70.65% to 47.53%, and down to 4.23% (Figure 17) eventually at normal pH value. On the contrary, the content of *Acidithiobacillus thiooxidans* increased through the leaching period. However, there was a slight decrease of the content of *Acidithiobacillus thiooxidans* along with the recession of *Acidithiobacillus ferrooxidans* at elevated pH value. It is also worth noting that both *Leptospirillum ferrooxidans* and *Ferrimicrobium acidiphilum* grew better at pH 3.00.

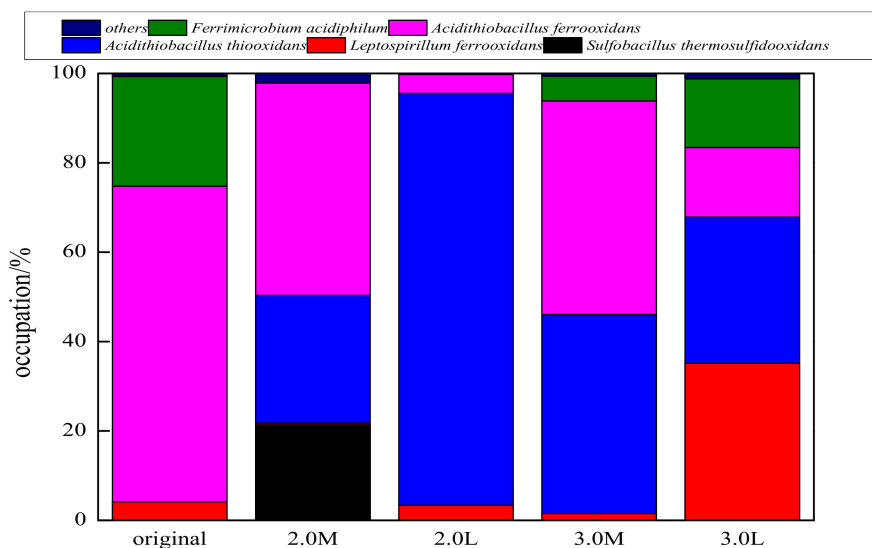


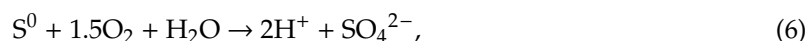
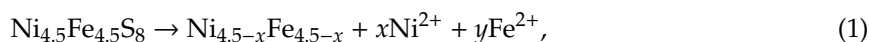
**Figure 17.** Bacterial community of the original leaching bacteria and leaching bacteria adsorbed on the leached samples (original: original leaching bacteria; 2.0 M: pH = 2.00, leached for 8 days; 2.0 L: pH = 2.00, leached for 16 days; 3.0 M: pH = 3.00, leached for 8 days; 3.0 L: pH = 3.00, leached for 16 days).

## 4. Discussion

### 4.1. The Oxidation and Decomposition Process of Pentlandite

According to the chemical leaching experiments with Fe<sup>3+</sup>, the non-uniform release of Ni<sup>2+</sup> and Fe<sup>2+</sup> confirms Equation (1), which could also lead to the formation of a metal-deficient (sulfur-rich)

surface layer.  $\text{Fe}^{2+}$  was released prior to  $\text{Ni}^{2+}$ . Meanwhile, the abiotic leaching test suggests that hydrogen ions benefit the dissolution of metal ions mainly due to the cleaving of the Fe-S and Ni-S bonding [11] (Equation (2)). However, both M-S and  $\text{H}_2\text{S}$  could be oxidized by  $\text{Fe}^{3+}$  or the leaching bacteria. Ferric ions have a prominent effect on the oxidation of  $\text{S}_2^{2-}$  and  $\text{S}^{2-}$  (Equations (3) and (4)) and the reduced ferrous ions could be re-oxidized back to  $\text{Fe}^{3+}$  by the leaching bacteria (Equation (5)). Elemental sulfur could hardly be oxidized by ferric ions, and it was confirmed as a crucial passivation product by many previous studies [18,19]. The oxidation of sulfur species could be divided into two categories: the formation of  $\text{S}^0$  during the oxidation of  $\text{S}_2^{2-}$  and  $\text{S}^{2-}$ , and the oxidation of  $\text{S}^0$ . The reduced sulfur species ( $\text{S}^{2-}$  and  $\text{S}_2^{2-}$ ) could be oxidized by both  $\text{Fe}^{3+}$  and the leaching bacteria. However, the oxidation of  $\text{S}^0$  is only remarkable when the sulfur-oxidizing microorganisms are presented (Equation (6)), as the chemical oxidation with dissolved oxygen could be ignored under low pH values. As another current reported passivation product, jarosite [20,21] was also found on the surface of the pentlandite particles. The formation of jarosite is mainly caused by the precipitation of ferric ions. According to Equation (7), more jarosite will generate when the concentration of hydrogen ions is low.



In all, the release of Ni and Fe atoms is accomplished with the oxidation of sulfur species and the formation of jarosite on the surface of the pentlandite particles. At the initial stage,  $\text{Ni}^{2+}$  and  $\text{Fe}^{2+}$  dissolve freely after the wetting of the fresh pentlandite surface. Yet with the dissolution of  $\text{Ni}^{2+}$  and  $\text{Fe}^{2+}$ , a hydrophobic, metal-deficient layer remained at the solid-liquid interface. The dissolved  $\text{Fe}^{2+}$  stimulates the growth of the leaching bacteria, and the metabolite  $\text{Fe}^{3+}$  could accelerate the transformation of  $\text{S}^{2-}/\text{S}_2^{2-}$ . With the depletion of  $\text{Fe}^{2+}$ , a high Eh value was maintained despite the continual participation of  $\text{Fe}^{3+}$ . As the process went on, a jarosite layer formed on the mineral surface covering the pentlandite grains.

#### 4.2. Fe, Ni and S Species Modification During the Oxidation and Decomposition of Pentlandite

During the bioleaching of pentlandite, Fe, Ni and S atoms show different transform pathways. In a bioleaching system, the target element is nickel. Nevertheless, the intermediate species may have adverse effect on the leaching of nickel. Hence, it is of vital importance to verify the modification pathways of Fe, Ni and S.

##### 4.2.1. Fe Modification

Within the experimental conditions, there are four kinds iron species detected during the bioleaching of pentlandite. It is obvious that  $\text{Fe}^{2+}$  is released directly after the break of Fe-S bond. Then  $\text{Fe}^{2+}$  is oxidized by the iron-oxidizing bacteria. The generated  $\text{Fe}^{3+}$  could be reduced during the oxidation of  $\text{S}^{2-}$  and  $\text{S}_2^{2-}$ .  $\text{Fe}^{3+}$  is continuously consumed during the formation of jarosite. Also, a reconstruction process was observed during the later stage of the chemical leaching experiment with  $\text{Fe}^{3+}$ . The X-ray diffraction pattern suggests that  $\text{FeS}_2$  appears on the surface of pentlandite particles. However, no evidence of this process was found when the leaching bacteria were presented. In all, the Fe modification pathway could be described as follows:



#### 4.2.2. Ni Modification

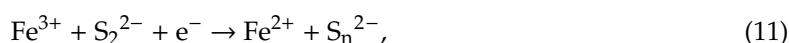
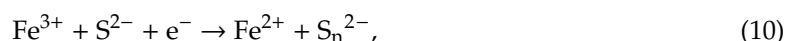
(Ni,Fe)<sub>9</sub>S<sub>8</sub>, NiS and Ni<sup>2+</sup> were detected as the nickel species despite bioleaching or chemical leaching systems, suggesting a Ni modification pathway as follows:



Comparing to chemical experiments, a significant acceleration was shown in the transformation from (Ni,Fe)<sub>9</sub>S<sub>8</sub> to NiS in the bioleaching experiments. According to Figures 2 and 8, more NiS appeared on the pentlandite surface when the Eh value increased from less than 450 mV to nearly 600 mV, indicating a positive impact of high Eh value.

#### 4.2.3. S Modification

The detection of S<sup>2-</sup> and S<sub>2</sub><sup>2-</sup> suggested the existence of four-coordinate S and five-coordinate S [22] on the pentlandite surface. The peaks at about 163.6 eV to 163.9 eV represent S<sub>n</sub><sup>2-</sup>, implying a two-step reaction during the formation of S<sup>0</sup>.



Throughout all the leaching experiments, no evidence of S<sub>2</sub>O<sub>3</sub><sup>2-</sup> was found. The absence of S<sub>2</sub>O<sub>3</sub><sup>2-</sup> and the presence of S<sub>n</sub><sup>2-</sup> and S<sup>0</sup> indicate that sulfur was modified through the polysulfide mechanism [23] during the bioleaching of pentlandite. SO<sub>3</sub><sup>2-</sup> was undetectable mainly due to its high reactivity. The S modification pathway could be described as follows:



#### 4.3. Conceptual Model of the Oxidation and Decomposition of Pentlandite

A conceptual model of the oxidation and decomposition of pentlandite during the bioleaching process is proposed by integrating the results within this work (Figures 18 and 19). The model consists of two kinds leaching microorganisms (iron-oxidizing and sulfur-oxidizing microorganisms) with different metabolic systems and three pathways of element modification (Ni, Fe and S).

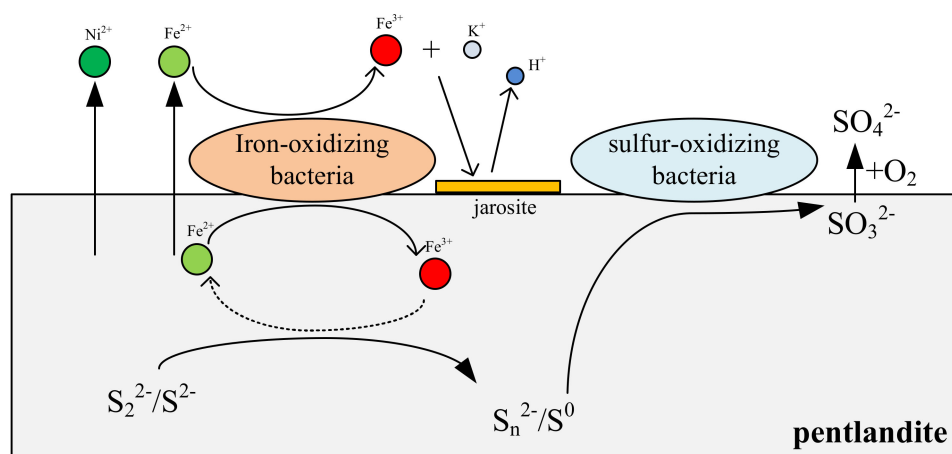


**Figure 18.** Conceptual model for the oxidation and decomposition of pentlandite during bioleaching with iron- and sulfur-oxidizing microorganisms.

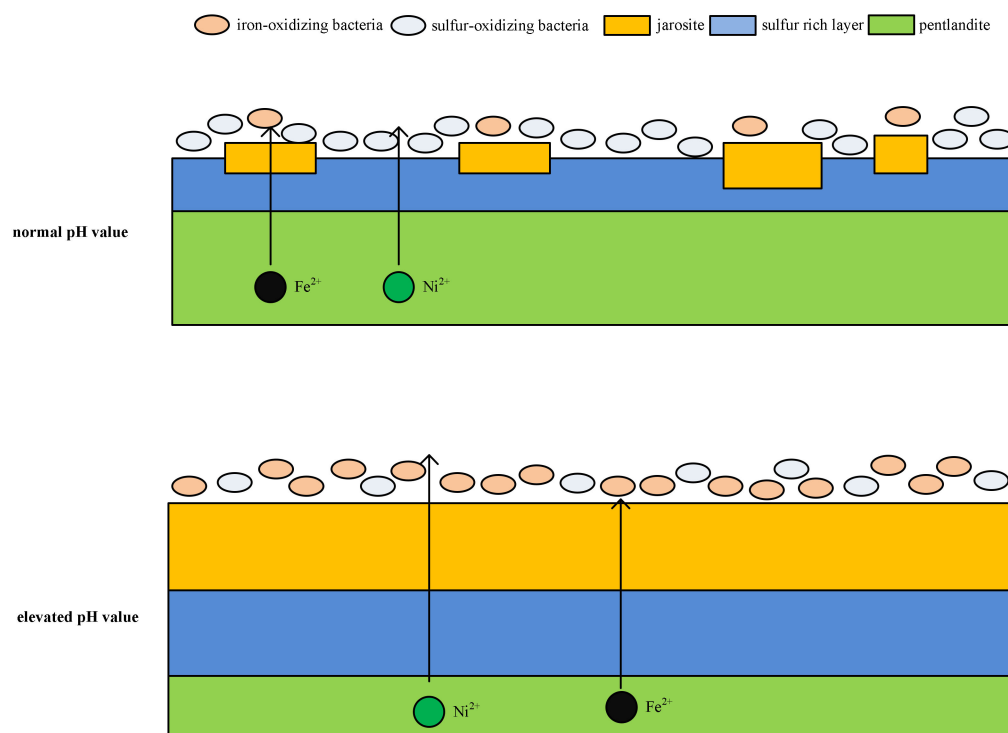


**Figure 19.** Differences of mineral and leaching bacteria behaviors during pentlandite bioleaching with normal and elevated pH values.

Pentlandite particles are affirmed as the major energy resource for the leaching bacteria, and most leaching bacteria will adsorb on the mineral surface. The adsorption of leaching bacteria is of crucial importance to the bioleaching of pentlandite, and it could further evidence the contact mechanism [24]. The iron-oxidizing and sulfur-oxidizing microorganisms changed the chemical solution and mineral surface of the pentlandite leaching system. Iron-oxidizing microorganisms (*Leptospirillum ferrooxidans*) could obtain energy from  $\text{Fe}^{2+}$  oxidation with electron transfer pathway [25] and accelerate the generation of  $\text{Fe}^{3+}$ , which will further promote the oxidation of  $\text{S}_2^{2-}$  and  $\text{S}^{2-}$ . However, sulfur-oxidizing microorganisms (*Acidithiobacillus thiooxidans*) could only obtain energy from inorganic sulfur compounds [26]. Hence, the surface microbial community succeeds with the consumption of  $\text{Fe}^{2+}$  and reduction sulfur species. The presence of *Leptospirillum ferrooxidans* and *Acidithiobacillus thiooxidans* suggests the existence of available  $\text{Fe}^{2+}$  and reduction in sulfur species. At normal pH value (pH = 2.00), the recession of *Acidithiobacillus ferrooxidans* and the growth of *Acidithiobacillus thiooxidans* in the later stage implies the consumption of  $\text{Fe}^{2+}$  and the enrichment of reduction sulfur species. It is in agreement with the formation of the sulfur-rich layer caused by the release of metal ions. The community succession of the surface microorganisms indicates the preferential oxidation of  $\text{Fe}^{2+}$  over sulfur species. It also suggests that *Acidithiobacillus ferrooxidans* shows weaker competitive capacity comparing to *Acidithiobacillus thiooxidans* and *Leptospirillum ferrooxidans*. However, at elevated pH values (pH = 3.00), there is a slight recession of *Acidithiobacillus thiooxidans*, which suggests the coverage of jarosite on the reduced sulfur species. The coverage of jarosite hinders contact between sulfur-oxidizing microorganisms and reduced sulfur species. This will cause the accumulation of  $\text{S}^0$  as the further oxidation of element sulfur and is only significant when sulfur-oxidizing microorganisms are present. In general, it could be concluded that there are two kinds of product layers during the bioleaching of pentlandite: the inner sulfur-rich layer and the outer jarosite layer. According to the discussion above, formation of the jarosite layer will inhibit oxidation of the sulfur-rich layer. In that case, coverage of the jarosite layer will cause the accumulation of reduced sulfur species, and rise in pH will promote the process.

Another noteworthy point is the adsorption of an iron-oxidizing microorganism (*Leptospirillum ferrooxidans*) manifesting the existence of  $\text{Fe}^{2+}$  on the surface of the pentlandite particles during the later stage at pH 3.00. The adsorption of *Leptospirillum ferrooxidans* indicates that ferrous ions could transfer through the two product layers and get to the particle surface. It suggests that the inhibition of product layers on the dissolution of  $\text{Ni}^{2+}$  is non-significant, as the radius of  $\text{Ni}^{2+}$  is smaller than that of  $\text{Fe}^{2+}$ . This could be a major point in nickel bioleaching from pentlandite at elevated pH values.

#### 4.4. Implications for Hydrometallurgical Applications in the Nickel Industry

In all, the oxidation and decomposition of pentlandite is promoted by the combination of  $\text{Fe}^{3+}$ ,  $\text{H}^+$ ,  $\text{O}_2$  and leaching bacteria. According to Figure 12, a similar nickel leaching efficiency was achieved at both elevated (pH = 3.00) and normal (pH = 2.00) pH values. The results correspond with Cameron's work [27]. Tested with six pentlandite-bearing sulfide ores, a similar nickel leaching efficiency was achieved at both pH 2.00 and 3.00. Unlike chalcopyrite [28] and pyrite [29], the bioleaching of nickel from pentlandite could be achieved with a lower concentration of  $\text{Fe}^{3+}$  and higher pH value. Most pentlandite-bearing ores are associated with magnesium-bearing silicate gangue mineral such as olivine and serpentine. According to other research before, an elevated pH value is beneficial to inhibit  $\text{Mg}^{2+}$  dissolution from magnesium-bearing minerals [30,31]. Combining these two points, it may be possible to achieve a considerable nickel leaching efficiency with less dissolution of  $\text{Mg}^{2+}$  and acid consumption. However, further studies about detailed engineering parameters, especially pH values, are still needed.

## 5. Conclusions

A comprehensive study about the effect of  $\text{Fe}^{3+}$ ,  $\text{H}^+$  and leaching bacteria on the oxidation and decomposition of pentlandite was carried out. It is suggested that they could enhance the leaching of pentlandite in different degrees. Protons are beneficial in breaking M-S bonds.  $\text{Fe}^{3+}$  could promote the oxidation of  $\text{S}^{2-}$  and  $\text{S}_n^{2-}$ . Iron and sulfur-oxidizing microorganisms play different roles during bioleaching. Iron-oxidizing microorganisms could promote the generation of  $\text{Fe}^{3+}$  greatly. Sulfur-oxidizing microorganisms are crucial for the oxidation of  $\text{S}_n^{2-}$  and  $\text{S}^0$ . Iron in the pentlandite transformed through a  $(\text{Ni,Fe})_9\text{S}_8 \rightarrow \text{Fe}^{2+} \rightarrow \text{Fe}^{3+} \rightarrow \text{KFe}_3(\text{SO}_4)_2(\text{OH})_6$  pathway. Nickel in the pentlandite experienced a transformation from  $(\text{Ni,Fe})_9\text{S}_8$  to  $\text{NiS}$ , and it finally released to the solution as  $\text{Ni}^{2+}$ . The sulfur species in pentlandite was modified through the polysulfide mechanism, which is  $\text{S}^{2-}/\text{S}_2^{2-} \rightarrow \text{S}_n^{2-} \rightarrow \text{S}^0 \rightarrow \text{SO}_3^{2-} \rightarrow \text{SO}_4^{2-}$ . There are two product layers on the pentlandite particles during bioleaching, but they showed non-significant inhibition on the dissolution of  $\text{Ni}^{2+}$ . Hence, it could be possible to bioleach pentlandite at an elevated pH value, inhibiting the dissolution of  $\text{Fe}^{3+}$  and  $\text{Mg}^{2+}$  from ore.

**Author Contributions:** Conceptualization, J.S. and J.W.; Data curation, J.S.; Formal analysis, J.S. and B.W.; Funding acquisition, B.C.; Investigation, J.S.; Methodology, J.S.; Project administration, B.W.; Resources, B.W.; Software, J.S. and B.C.; Supervision, J.W.; Validation, J.W.; Visualization, B.W.; Writing—original draft, J.S.; Writing—review & editing, J.S., J.W. and B.C. All authors have read and agreed to the published version of the manuscript.

**Funding:** This research was funded by National Natural Science Foundation of China (No. 51574036, No 51704028 and No. 51404033) and Key research and development plan of Yunnan province (No. 2018IB027).

**Acknowledgments:** The authors are grateful to all the members of the National Engineering Laboratory of Biohydrometallurgy, GRINM Group Corporation Limited, China.

**Conflicts of Interest:** The authors declare no conflicts of interest. The funders had no role in the design of the study; in the collection, analyses, or interpretation of data; in the writing of the manuscript, or in the decision to publish the results.

## References

1. Riekkola-Vanhanen, M. Talvivaara mining company—From a project to a mine. *Miner. Eng.* **2013**, *48*, 2–9. [[CrossRef](#)]
2. Halinen, A.K.; Rahunen, N.; Kaksonen, A.H.; Puhakka, J.A. Heap bioleaching of a complex sulfide ore: Part I: Effect of pH on metal extraction and microbial composition in pH controlled columns. *Hydrometallurgy* **2009**, *98*, 92–100. [[CrossRef](#)]
3. Arpalahti, A.; Lundström, M. The leaching behavior of minerals from a pyrrhotite-rich pentlandite ore during heap leaching. *Miner. Eng.* **2018**, *119*, 116–125. [[CrossRef](#)]
4. Zhen, S.J.; Qin, W.Q.; Yan, Z.Q.; Zhang, Y.S.; Wang, J.; Ren, L.Y. Bioleaching of low grade nickel sulfide mineral in column reactor. *Trans. Nonferrous Met. Soc. China.* **2008**, *18*, 1480–1484. [[CrossRef](#)]
5. Zhen, S.; Yan, Z.; Zhang, Y.; Wang, J.; Campbell, M.; Qin, W. Column bioleaching of a low grade nickel-bearing sulfide ore containing high magnesium as olivine, chlorite and antigorite. *Hydrometallurgy* **2009**, *96*, 337–341. [[CrossRef](#)]
6. Lu, Z.Y.; Jeffrey, M.I.; Zhu, Y.; Lawson, F. Studies of pentlandite leaching in mixed oxygenated acidic chloride-sulfate solutions. *Hydrometallurgy* **2000**, *56*, 63–74. [[CrossRef](#)]
7. Baláž, P.; Boldižárová, E.; Achimovičová, M.; Kammel, R. Leaching and dissolution of a pentlandite concentrate pretreated by mechanical activation. *Hydrometallurgy* **2000**, *57*, 85–96. [[CrossRef](#)]
8. Maurice, D.; Hawk, J.A. Ferric chloride leaching of a mechanically activated pentlandite–chalcopyrite concentrate. *Hydrometallurgy* **1999**, *52*, 289–312. [[CrossRef](#)]
9. Fu, B.; Zhou, H.; Zhang, R.; Qiu, G. Bioleaching of chalcopyrite by pure and mixed cultures of *Acidithiobacillus* spp. and *Leptospirillum ferriphilum*. *Inter. Biodeterior. Biodegrad.* **2008**, *62*, 109–115. [[CrossRef](#)]
10. Leão, V.A.; Cruz, F.L.S.; Oliveira, V.A.; Guimarães, D.; Souza, A.D. High-temperature bioleaching of nickel sulfides: Thermodynamic and kinetic implications. *Hydrometallurgy* **2010**, *105*, 103–109. [[CrossRef](#)]
11. Sand, W.; Gehrke, T.; Jozsa, P.G.; Schippers, A. (Bio)chemistry of bacterial leaching—Direct vs. indirect bioleaching. *Hydrometallurgy* **2001**, *59*, 159–175. [[CrossRef](#)]
12. Holmes, D.S.; Eugenia, J.; Yann, D.; Corinne, A.A.; Raquel, Q.; Violaine, B. Extending the models for iron and sulfur oxidation in the extreme Acidophile *Acidithiobacillus ferrooxidans*. *BMC Genomics* **2009**, *10*, 394. [[CrossRef](#)]
13. Dorado, A.D.; Solé, M.; Lao, C.; Alfonso, P.; Gamisans, X. Effect of pH and Fe(III) ions on chalcopyrite bioleaching by an adapted consortium from biogas sweetening. *Miner. Eng.* **2012**, *39*, 36–38. [[CrossRef](#)]
14. Li, Q.; Tian, Y.; Fu, X.; Yin, H.; Zhou, Z.; Liang, Y.; Qiu, G.; Liu, J.; Liu, H.; Liang, Y.; et al. The Community Dynamics of Major Bioleaching Microorganisms During Chalcopyrite Leaching Under the Effect of Organics. *Curr. Microbiol.* **2011**, *63*, 164–172. [[CrossRef](#)] [[PubMed](#)]
15. Cameron, R.A.; Lastra, R.; Gould, W.D.; Mortazavi, S.; Thibault, Y.; Bedard, P.L.; Morin, L.; Koren, D.W.; Kennedy, K.J. Bioleaching of six nickel sulphide ores with differing mineralogies in stirred-tank reactors at 30 °C. *Miner. Eng.* **2013**, *49*, 172–183. [[CrossRef](#)]
16. Simon, A.; Paul, T.P.; Wolfgang, H. HTSeq—A Python framework to work with high-throughput sequencing data. *Bioinformatics* **2015**, *31*, 166–169. [[CrossRef](#)]
17. Meruane, G.; Vargas, T. Bacterial oxidation of ferrous iron by *Acidithiobacillus ferrooxidans* in the pH range 2.5–7.0. *Hydrometallurgy* **2003**, *71*, 149–158. [[CrossRef](#)]
18. Zhang, R.; Wei, D.; Shen, Y.; Liu, W.; Tao, L.; Cong, H. Catalytic effect of polyethylene glycol on sulfur oxidation in chalcopyrite bioleaching by *Acidithiobacillus ferrooxidans*. *Miner. Eng.* **2016**, *95*, 74–78. [[CrossRef](#)]
19. Wu, S.F.; Yang, C.R.; Qin, W.Q.; Jiao, F.; Wang, J.; Zhang, Y.S. Sulfur composition on surface of chalcopyrite during its bioleaching at 50 °C. *Trans. Nonferrous Met. Soc.* **2015**, *25*, 4110–4118. [[CrossRef](#)]
20. Pan, H.D.; Yang, H.Y.; Tong, L.L.; Zhong, C.B.; Zhao, Y.S. Control method of chalcopyrite passivation in bioleaching. *Trans. Nonferrous Met. Soc. China* **2012**, *22*, 2255–2260. [[CrossRef](#)]
21. Huang, C.; Qin, C.; Feng, X.; Liu, X.; Tao, J. Chalcopyrite bioleaching of an in situ leaching system by introducing different functional oxidizers. *RSC Adv.* **2018**, *8*, 37040–37049. [[CrossRef](#)]
22. Legrand, D.L. Oxidation/alteration of pentlandite and pyrrhotite surfaces at pH 9.3: Part 1. Assignment of XPS spectra and chemical trends. *Am. Mineral.* **2005**, *90*, 1042–1054. [[CrossRef](#)]
23. Tao, H.; Li, D. Presentation on mechanisms and applications of chalcopyrite and pyrite bioleaching in biohydrometallurgy—A presentation. *Biotechnol. Rep.* **2014**, *4*, 107–119. [[CrossRef](#)]

24. Tributsch, H. Direct versus indirect bioleaching. *Hydrometallurgy* **2001**, *59*, 177–185. [[CrossRef](#)]
25. Zhang, S.; Yan, L.; Xing, W.; Chen, P.; Zhang, Y.; Wang, W. *Acidithiobacillus ferrooxidans* and its potential application. *Extremophiles* **2018**, *22*, 563–579. [[CrossRef](#)] [[PubMed](#)]
26. Jorge, V.; Francisco, O.; Raquel, Q.; Mark, D.; Holmes, D.S. Draft genome sequence of the extremely acidophilic biomining bacterium *Acidithiobacillus thiooxidans* ATCC 19377 provides insights into the evolution of the *Acidithiobacillus* genus. *J. Bacteriol.* **2011**, *193*, 7003–7004. [[CrossRef](#)]
27. Cameron, R.A.; Lastra, R.; Mortazavi, S.; Gould, W.D.; Thibault, Y.; Bedard, P.L.; Morin, L.; Kennedy, K.J. Elevated-pH bioleaching of a low-grade ultramafic nickel sulphide ore in stirred-tank reactors at 5 to 45 °C. *Hydrometallurgy* **2009**, *99*, 77–83. [[CrossRef](#)]
28. Liu, H.C.; Nie, Z.Y.; Xia, J.L.; Zhu, H.R.; Yun, Y.; Zhao, C.H.; Lei, Z.; Zhao, Y.D. Investigation of copper, iron and sulfur speciation during bioleaching of chalcopyrite by moderate thermophile *Sulfobacillus thermosulfidooxidans*. *Int. J. Miner. Process.* **2015**, *137*, 1–8. [[CrossRef](#)]
29. Li, J.; Lu, J.; Lu, X.; Tu, B.; Ouyang, B.; Han, X.; Wang, R. Sulfur transformation in microbially mediated pyrite oxidation by: Insights from X-ray photoelectron spectroscopy-based quantitative depth profiling. *Geomicrobiology* **2015**, *33*, 118–134. [[CrossRef](#)]
30. Daval, D.; Hellmann, R.; Martinez, I.; Gangloff, S.; Guyot, F. Lizardite serpentine dissolution kinetics as a function of pH and temperature, including effects of elevated pCO<sub>2</sub>. *Chem. Geol.* **2013**, *351*, 245–256. [[CrossRef](#)]
31. Crundwell, F.K. The mechanism of dissolution of forsterite, olivine and minerals of the orthosilicate group. *Hydrometallurgy* **2014**, *150*, 68–82. [[CrossRef](#)]



© 2020 by the authors. Licensee MDPI, Basel, Switzerland. This article is an open access article distributed under the terms and conditions of the Creative Commons Attribution (CC BY) license (<http://creativecommons.org/licenses/by/4.0/>).